International Journal of Science and Research (IJSR)
ISSN (Online): 2319-7064
Impact Factor (2012): 3.358

Characterization, AC Conductivity and Dielectric behaviour of Chemically Synthesized Poly Meta-Aminophenol

Thenmozhi G[1], Jaya Santhi R[2*]

P G & Research Department of Chemistry, Auxilium College, Vellore-632006, Tamil Nadu, India

Abstract: ***Substituted polyaniline, poly (m-aminophenol) was synthesized by oxidative chemical polymerization method using ammonium persulfate as an oxidant in an acidic medium at room temperature. The synthesized polymer was characterized by GPC, UV-VIS-NIR, FT-IR, ^{1}H NMR, XRD, SEM and TGA-DTA. The AC electrical conductivity and dielectric behavior was investigated using complex impedance spectroscopy over the frequency range of 20Hz–10^{6}Hz and in the temperature range of 303–383K. AC conductivity is found to increases with increase of temperatures. In the entire range, the universal power law $\sigma_{ac}\omega=A\omega^S$ holds well. The polymer displays a decrease in frequency exponent 'S' value in the entire temperature range of study and hence follow Correlated Barrier Hopping (CBH) conduction mechanisms. Both dielectric constant and dielectric loss increases with the decrease of frequency exhibiting strong interfacial polarization at low frequency. At higher frequencies PMAP exhibits almost zero dielectric loss which suggests that this polymer is lossless material at frequencies beyond 10^{5}Hz. Complex electric modulus and dissipation factor exhibits two relaxation peaks, indicating two-phase structure as indicated by a bimodal distribution of relaxation process.***

Keywords: Aminophenol, Polymerization, AC conductivity, Dielectric behavior, Activation energy.

1. Introduction

The conducting polymers have wide applications such as solar cells, lightweight batteries, light emitting diodes, polymer actuators, corrosion protection agents, sensors and molecular electronic devices [1]. A derivative of polyaniline, Amino phenols are interesting electrochemical materials since, unlike aniline and other substituted anilines, they have two groups (–NH_2 and –OH) which can be oxidized. Therefore, they can show electrochemical behaviour resembling anilines and phenols [2]. In recent years, electrical and optical properties of conducting polymers like polyaniline and substituted polyaniline synthesized by chemical oxidation polymerization have been studied in great detail. Impedance spectroscopy is a very useful technique in solid state electronic system, because it can resolve the conduction components by differentiating between the transports properties of complex systems [3]. Conducting polymers are highly disordered materials for which the enhancement of conductivity on doping / dedoping comes from the generation of extended states in doped molecules correlating charged defects with electronic structures. Measurements of AC conductivity have been extensively used to understand the conduction process in insulating materials. Various models have been proposed to explain the AC conduction mechanism. These models were more particularly developed to understand the mechanisms of electric conduction in disordered materials, such as amorphous semiconductors, ionic conductive glasses, ionic or electronic conducting polymers, organic semiconductors and non stoichiometric or highly defective crystals. The behavior of AC conductivity according to the frequency and the temperature generally follows a similar behavior in all these disordered solids [4]. In the present work, Poly Meta Aminophenol (PMAP) was synthesized by chemical oxidation method and characterized by different spectroscopic techniques. The complex impedance spectroscopy is a powerful tool for the study of electrical properties such as bulk resistance, bulk AC conductivity and dielectric properties, etc., particularly of semiconducting materials. An attempt is made herein to study these electrical properties of PMAP material as a function of frequency and temperature. Interesting results are observed from frequency and temperature-dependent AC conductivity and dielectric response of the synthesized polymer.

2. Experimental Method

2.1 Synthesis of poly Meta aminophenol

The PMAP was synthesized in acidic medium using ammonium persulfate by following our earlier descried method [5]. 0.1M m-aminophenol and 1M Hcl were taken in a beaker containing 50 ml toluene. Polymerization reaction was started by drop wise addition of aqueous solution of APS and the reaction was carried out for 12 h at room temperature with constant stirring. Polymerization was stopped by addition of 50 ml methanol. The PMAP precipitated was filtrated and washed with methanol and acetone. The powder of PMAP was then dried at 50˚C for 24h.

2.2 Characterization

Molecular weight was determined by gel permeation chromatography using Styragel columns and a refractive detector (Waters, model R 4000) with THF as the mobile phase. Carbon-Hydrogen-Nitrogen analysis of PMAP was carried out by a micro analytical technique using an Elementar Vario EL 3 elemental analyzer. UV/VIS/NIR spectra of PMAP dissolved in DMSO solvent was obtained using Varian, Cary-5000 spectrophotometer in the range of 200-2500 nm. The FT-IR spectrum of PMAP was recorded by Thermo Nicolet, Avatar 370 Spectrophotometer. The spectrum of the dry polymer powder in KBr pellet was recorded from 500cm^{-1} to 4000cm^{-1}. ^{1}H NMR spectra of

PMAP was recorded in a Bruker (600 MHz) instrument using d_6-DMSO as solvent. X-ray diffraction (XRD) scan was done with Bruker AXS D8 Advance diffractometer at room temperature using Cu Kα (λ=1.5406 A˚). The 2θ angle range was from 0˚ to 70˚. Scanning Electron Microscopy (SEM) was obtained by JEOL JSM 6390LV for PMAP. Thermo gravimetric analysis (TGA-DTA) was carried out in nitrogen atmosphere at a heating rate 10˚C/min up to 750˚C temperature by Perkin Elmer, Diamond TG/DTA analyzer.

The electrical characterization measurements were made in the temperature range 303-383K by the complex impedance method using a Hewlett Packard model HP 4284A Precision LCR Meter in the frequency range 20 Hz to 10^6 Hz [6]

3. Results and Discussion

3.1 Molecular weight and Elemental analysis

The molecular weight of the soluble portion of the PMAP was determined by gel permeation chromatography performed in THF. The number-average molecular weight (M_n), weight-average molecular weight (M_w) and poly dispersity index (M_w/M_n) values were found to be 11349, 35562, and 3.13, respectively. Broad distribution of molecular weights, characterized by weight-to-number molecular weight ratio M_w/M_n = 3.13, suggests the presence of small amount of oligomers in the polymer sample.

The elemental analysis data of PMAP contains Carbon 59%, Hydrogen 4.9%, Nitrogen 7.6% and Sulfur 0.7%. Elemental analysis result indicates some Sulfur incorporates in PMAP due to the salt formation of liberated sulfuric acid from the reduction of oxidant APS with -N- present within the polymer chain [7].

3.2 UV-VIS-NIR Spectroscopy

UV/VIS/NIR absorption spectrum of PMAP dissolved in DMSO is shown in Figure 1. The spectrum consist of two major absorption peaks, the first peak at 285-305 nm (4.35-4.06eV) is assigned to the π − π* transition of the phenyl rings which is related to the extent of conjugation between the phenyl rings in the polymer chain. The extended conjugation of π orbital is said to be responsible for conductivity which requires coplanarity of the atoms involved in π-electron delocalization for maximum resonance interaction [8]. The second absorption peak at 565–610 nm shows n-π* transitions within the quinoid structure [9]. The wavelength of the quinoid peak plays an important role in switching PMAP from an electric insulator to a conductor upon doping. The peak at 825 nm (1.5eV) has been assigned to $–NH_2^+–$ species which is generated on doping or the polaronic transitions.

3.3 FT-IR Analysis

The representative FT- IR spectrum of PMAP is given in Figure 2. A broad peak appears in the region 3600–1800 cm^{-1} is due to the stretching of aromatic C–H, hydrogen bonded –OH, and –NH– groups. The –OH group is hydrogen bonded with nearest nitrogen of –NH group present in the polymer chain through the H_2O molecule present in the sample. So –OH absorption peak appears at about 3333cm^{-1} as a broad peak. Two main peaks at 1600 and 1523cm^{-1} in the spectrum correspond respectively to the ring-stretching vibrations of the quinoid and benzenoid rings. The presence of these two rings clearly shows that the polymer is composed of the amine and imine units. The peak near 1285cm^{-1} is assigned to the C-N stretching adjacent to the quinoid structure. The peak appears at 2362cm^{-1} which is the characteristics stretching peak for C = C = N or C = C = O [10]. The peak at 1147 cm^{-1} is ascribed to the stretching of the C - O - C linkages [11] and further support that the m-aminophenol changed into PMAP. The peaks at 690, 769, and 831 cm^{-1} corresponded to the ortho and para disubstitutions in the benzene rings.

3.4 ^{1}H NMR Spectrum

Figure 3 shows the ^{1}H NMR spectrum of PMAP. The signals in the region of δ 6 - 7.8 correspond to the protons of the aromatic rings. The terminal $–NH_2$ groups in the compound give a very weak peak at δ 5.6 as singlet [9]. A peak of the OH proton in phenol in DMSO occurs at δ 9.2. Therefore, the peak at δ 8.9 is due to the OH proton in PMAP [12] and δ 8.4 is due to –NH– present in the polymer. Two signals at δ 2.48 and δ 3.35 arises from the protons present in$–CH_3$ group of DMSO and residual water in the sample as well as in the solvent. This NMR result is in agreement with that of UV-VIS-NIR and FT-IR spectrum of PMAP.

3.5 XRD Analysis and Morphology

Figure 4 shows the X-ray diffraction patterns of PMAP. The diffraction patterns were typical of crystalline / amorphous polymer. The crystalline regions in the PMAP are shown by the presence of relatively sharp peaks. The amorphous regions are visible by the broad low intensity peaks. The PMAP exhibits five broad peaks at 2θ angles around 53.8˚, 40.8˚, 35.54˚, 27.02˚ and 5.07˚, 2θ=27˚ is characteristics of the van der Waals distances between stacks of phenylene rings (poly aminophenol rings). These broad peaks indicate crystalline domains in the amorphous structure of PMAP. The degree of crystalline or ordered structural pattern in PMAP is due to the more intra chain hydrogen bonding or electrostatic interaction (through both amine and/or phenolic group). The SEM micrograph was used to investigate the morphology of the PMAP and shown in figure 5. The PMAP display two features, one of amorphous and the other of crystalline domain. The crystalline morphology may result from intra molecular hydrogen bonded amino phenol units. The particles are sharp edged with lamellar structure on one side and in amorphous side there are no well defined shapes. This result was supported as above from the X-ray diffraction patterns of PMAP.

3.6 Thermo Gravimetric Analysis

The TGA and DTA thermograms of PMAP are shown in Figure 6 and exhibit a three stage decomposition pattern.

The first stage of weight loss (wt.5.6 %) starts from 68 to115˚C corresponds to loss of water molecules / moisture and volatilization of the solvent. The second stage weight loss (wt.21.7 %) occurs between 150 and 220˚C and may be attributed to the loss of acid dopant bound to the polymer chain. The third stage weight loss (wt.43.7%) occurs between 265 and 368˚C is due to the complete degradation and decomposition of the polymer backbone. The first exothermic peak around 65˚C in the DTA curve correlates to the loss of adsorbed Hcl and moisture in the TG study. The endothermic peak between 190 and 225˚C can be attributed to the morphological changes and disruption of inter and intra molecular hydrogen bonding and loss of dopant. The second broad exotherm denoting the final degradation step occurs around 365˚C.

3.7 AC Conductivity

Figure 7 shows the complex impedance plots obtained for PMAP measured at nine different temperatures like 303, 313, 323, 333, 343, 353, 363,373 and 383 K respectively. It is observed from fig.7 that the impedance plots are found to show the presence of a low frequency arc, which arises due to the effect of electrode polarization and is incomplete in the frequency range, studied. The value of bulk resistance at these temperatures was estimated from the intersection point of the high frequency semicircles on the real axis. The temperature dependant Ac conductivity value for PMAP reveals that, the conductivity increases with temperature. The increase in conductivity with increase in temperature is the characteristic of 'thermal-activated behaviour' [13].

The temperature-dependent conductivity data obtained for PMAP over the temperature range 303–383 K are shown in Figure 8. It is interesting to note from fig.8 that the value of electrical conductivity (σ) increases with increasing temperature and the plot satisfy the Arrhenius equation $\sigma T = \sigma_0 \exp(-Ea/KT)$. Where σ_0 denotes the pre-exponential factor, Ea is the energy of activation for conduction and k is the Boltzmann constant. The activation energy was calculated from the slope of the observed linear plot drawn by the least square method and found to be 0.07eV.

In the study of frequency dependence of AC conductivity for PMAP log (σ) versus log (ω) plot was drawn and shown in Figure 9. The frequency dependence of the Ac conductivity follows a power law behavior. The total ac conductivity (σ'(ω)) can be represented by the equation $\sigma'(\omega) = \sigma_0 + \sigma_{ac}(\omega) = \sigma_{dc} + A\omega^S$ where ω is the angular frequency, σ_{dc} is the independent frequency conductivity or dc conductivity , A is the constant dependent on temperature T and S is an exponent dependent on both frequency and temperature with values in the range 0 - 1. This type of behaviour was noted by Jonscher, who called it as the "Universal Dynamic Response" (UDR) [14] because of a wide variety of materials that displayed such behavior.

From fig. 9, a linear increase in conductivity with frequency is noticed and the value of the frequency exponent S is estimated from the slope of the graph drawn with log (σ) versus log (ω), which is fully consistent with the power law. The dc conductivity value has also been calculated by extrapolating the ac conductivity data to zero frequency region and both S and dc conductivity values are presented in Table 1. The dc conductivity increases with increase in temperatures. It is observed from the table 1 that the estimated values of 'S' gradually decreases with increasing temperature for PMAP which satisfies the Correlated Barrier Hopping (CBH) model [15]. Therefore, from the trend of change in 'S' with temperature, it may be concluded that the ac conductivity in the investigated temperature ranges from 303 to 383K for PMAP can be described by the CBH model. The frequency exponent (S) for such model is given by the equation $S = 1 - 6K_BT / (W_M\text{-}KT \ln(\omega\tau))$ [16], where W_M is the height of maximum barrier (or binding energy) and τ is the relaxation time. W_M is calculated from the linear line slope which is between 1-S and T. A value of W_M=0.19 eV is obtained for PMAP.

3.8 Dielectric Behavior

Figure 10(a, b) shows the variation of dielectric constant (ε′) and dielectric loss (ε″) as a function of frequency for PMAP in the temperature range of 303–383 K. It is observed that both ε′ and ε″ increase with the decrease in frequency at all temperatures. Generally at any particular frequency, the dielectric constant is found to increase with the increase of temperature. This behaviour is more pronounced at lower frequencies. The enhancement of dielectric constant with decrease of frequency reveals that the systems exhibit strong interfacial polarization at low frequency. The strong low frequency dispersion for ε′ and no loss peak for ε″ are characteristics of charge carrier systems. It is also observed that ε′ and ε″ increases with temperature ranging from 303-383K due to the decrease in resistance of the investigated polymer. Electron hopping is promoted by the low resistance and hence an increase in polarizability or larger ε′ is obtained. Fig 10b shows that at lower frequencies, the loss factor (ε''_{obs}) increases linearly with the decreasing of frequency. This result suggests that dc conductivity process is more significant than interfacial polarization in PMAP. The interfacial polarization equation not follows a linear behaviour at lower frequencies.

Figure 11 (a, b) shows the isothermal and isochronal dependence of M" with the frequency and temperature, respectively for PMAP. It exhibits two peaks in both isothermal and isochronal plots, indicating clearly two different relaxation processes. The bimodal nature of electric modulus concerning PMAP, this type of behaviour has been also reported by Soares et al. in Poly aniline doped with dodecyl benzene sulfonic acid [17]. The authors affirm that the occurrence of two relaxation peaks is due to the two-phase structure with different state of oxidation: the lower frequency peak is attributed to the phase containing chains with more oxidized repeat units (imine groups) whereas the higher frequency peak is related to the phase containing chains with more reduced repeat units (amine groups) [17]. The position of the two relaxations peak does not change strongly with temperature.

The position of the characteristic relaxation frequency, ω_{max}, in plots of M" vs log ω depends upon the conductivity relaxation time, according to the expression,

$\omega_{max} = 1/2\pi\tau$

Relaxation time (τ) is a temperature dependent factor and it decreases as the temperature increases as shown in table 1. So when T increases ω_{max} becomes larger. The same is observed in the present study. The complex plane diagram of the electric modulus for PMAP is illustrated in Figure 12. PMAP clearly exhibit two arcs corresponding to two relaxation process at different temperatures ranging from 303 to 383K , as also observed in M"(log ω) or M"(T). The arcs initiate from the origin and spread to different values of M' depending upon the temperatures. These curves do not form semicircles, which could correspond to the idealized Debye model with double relaxation time. They rather possess a shape of deformed arcs with their centres positioned below the horizontal axis.

The reduced plots of M" / $M"_{max}$ versus log (ω / ω_{max}) at different temperatures provide additional information regarding the molecular heterogeneity of the polymer. Figure 13 illustrate reduced plot for PMAP and show that the distribution of relaxation times are nearly the same over the temperature range from 303-373K. The shape of the reduced modulus spectra at different temperatures clearly signifies the temperature independence of the Distribution of Relaxation Times (DRT), in view of the heterogeneous nature of the present polymer. The physical significance of the temperature independent DRT is that the distribution of conductivities in the polymer is temperature independent [18].

The dissipation factor, tan δ, recorded as a function of frequency for PMAP is shown in Figure 14. The loss tangent decreases with increasing frequency. As noted earlier, high loss at low frequency in loss tangent may be attributed to DC conduction losses as in the case of dielectric constant and dielectric loss. At higher frequencies PMAP exhibits almost zero dielectric loss which suggests that this polymer is lossless material at frequencies beyond 10^5Hz. It is absorbed those two peaks in frequency dependence loss tangent plots, indicating clearly two different relaxation processes which are already confirmed by fig 11 (a, b).

4. Conclusion

Poly Meta Aminophenol has been successfully synthesized by chemical oxidative method and characterized by different spectroscopic techniques. It is observed from Complex Impedance measurements that Ac conductivity increases moderately with temperature and it has been interpreted as a power law of frequency. Variation of the frequency exponent 'S' as a function of temperature indicates that charge transport in PMAP follows the CBH mechanism. The dc conductivity obtained by fitting the experimental ac conductivity data reveals an increase in the conductivity with temperatures. The dielectric constant and dielectric loss decreases with an increase in frequency. The electric modulus and dissipation factor recorded as a function of frequency and temperature displays two relaxation processes. At higher frequencies PMAP exhibit low dielectric loss, which suggests that PMAP is lossless materials at frequencies beyond 10^5Hz. The observed behavior is consistent with conductivity and dielectric constant results.

References

[1] M.Gerard, A. Chaubey, and B.D. Malhotra, Biosensors and Bioelectronics, vol. 17, 345, 2001.
[2] Evrim Hur, Gozen Bereket, Berrin Duran, Derya Ozdemir, and Yucel Sahin, Progress in organic coatings, vol. 60, 153, 2007
[3] M. Nadeem, M.J. Akhtar, and M.N. Haque, Solid state communications, vol. 145, 263, 2008.
[4] Abdelkader Kah ouli, Alain Sylvestre, Fethi Jomni, Bechir Yangui, and Julien Legrand, Journal of Physical Chemistry A, vol. 116, 1051, 2012.
[5] G. Thenmozhi, P. Arockiasamy, and Jayasanthi Raj,International Journal of Electrochemistry, vol. 2014, Article ID 961617, 11 pages, 2014.
[6] Thenmozhi Gopalasamy, Mohanraj Gopalswamy, Madhusudhana Gopichand, and Jayasanthi Raj,Journal of polymers, vol. 2014, Article ID 827043, 11 pages, 2014.
[7] P. Kar, N.C. Pradhan, and B. Adhikar, Materials Chemistry and Physics, vol. 111, 59, 2008
[8] H.S.O. Chan, S.C. Ng, W.S. Sim, K.L. Tan, and B.T.G. Tan,Macromolecules, vol. 25, 6029, 1992.
[9] A.G. Yavuz, and A. Gok, Synthetic Metals, vol. 157, 235, 2007.
[10] P. Kar, N.C. Pradhan, and B. Adhikar, Synthetic Metals, vol. 160, 1524, 2010.
[11] A. Ehsani, M.G. Mahjani, and M. Jafarian, Synthetic Metals, vol.162,1994, 2012.
[12] Jing Zhang, Dan Shan, and Shaolin Mu, Polymer, vol. 48, 1269, 2007.
[13] P. Chithra Lekha, D. Pathinettam Padiyan, Journal of Material Science, vol. 44, 6040, 2009.
[14] A.K. Jonscher, Nature, vol. 267,673, 1977.
[15] K. Gupta, G. Chakraborty, P.C. Jana, and A.K. Meikap, Solid State Communications, Vol. 151, 573, 2011.
[16] P. Dutta, S. Biskas, M. Ghosh, S. De, and S. Chatterjee, Synthetic metals, vol. 122, 455,2001.
[17] B.G. Soares,Maria, Elena Leyva, G. M.O. Barra, and Dipak Khastgir, European polymer journal, vol.42,676, 2006.
[18] S.A.Suthanthiraraj, and Y.D. Premchand, Journal of solid state chemistry, vol. 170, 142, 2003.

Figures and Tables

Table 1: Frequency Exponent (S), DC Conductivity and Relaxation Time (τ) of PMAP over the temperature range 303-383K

Temperature (K)	*S*	*DC Conductivity* $\times 10^{-7}$ *(S cm^{-1})*	*Relaxation Time (μ s)*
303	0.99	1.12	2.80
313	0.97	1.29	2.47
323	0.95	1.41	2.42
333	0.81	2.63	2.05
343	0.80	3.80	2.03
353	0.78	3.98	1.69
363	0.76	4.47	0.50
373	0.68	7.24	0.36
383	0.66	8.13	0.30

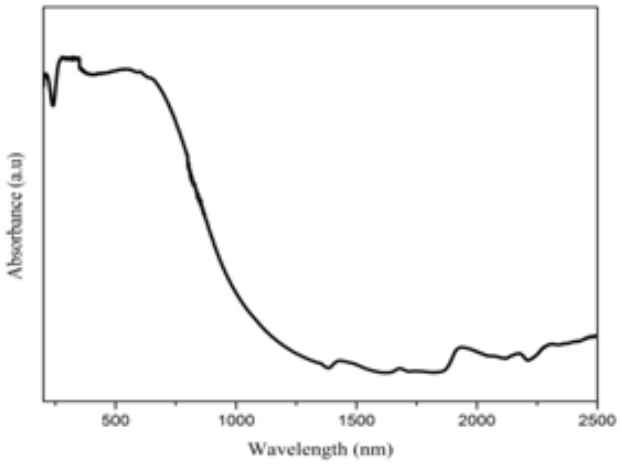

Figure 1: UV-VIS-NIR Spectra of PMAP in DMSO solvent

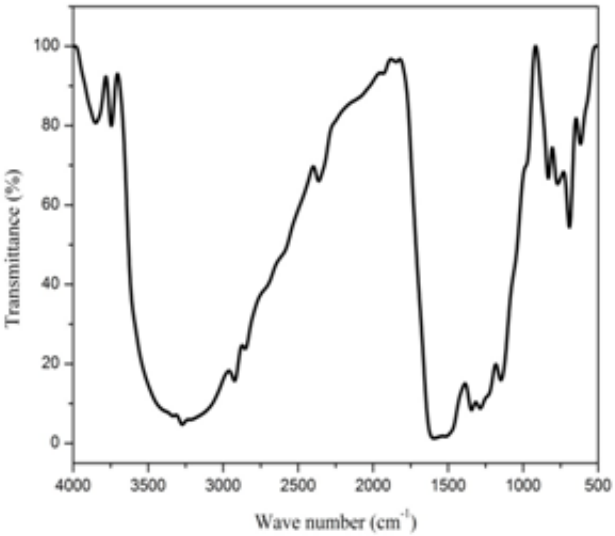

Figure 2: FT-IR Spectra of PMAP

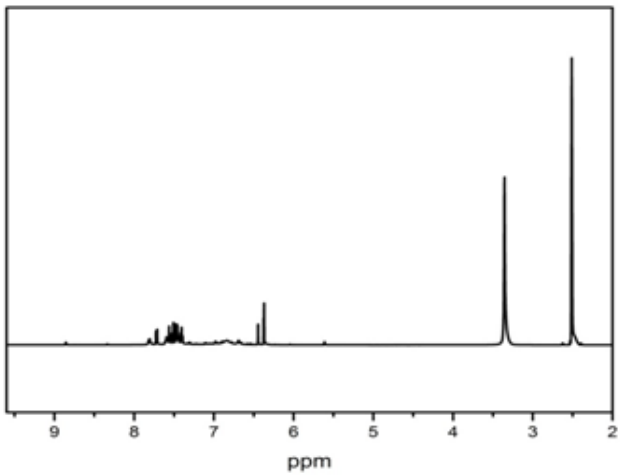

Figure 3: ^{1}H NMR Spectra of PMAP

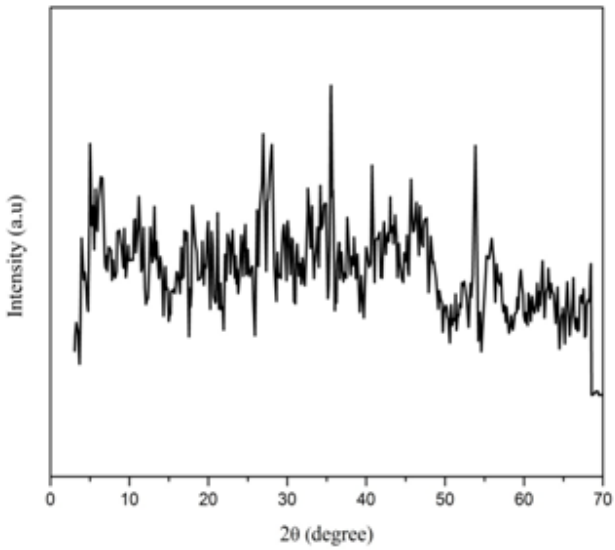

Figure 4: XRD Pattern of PMAP

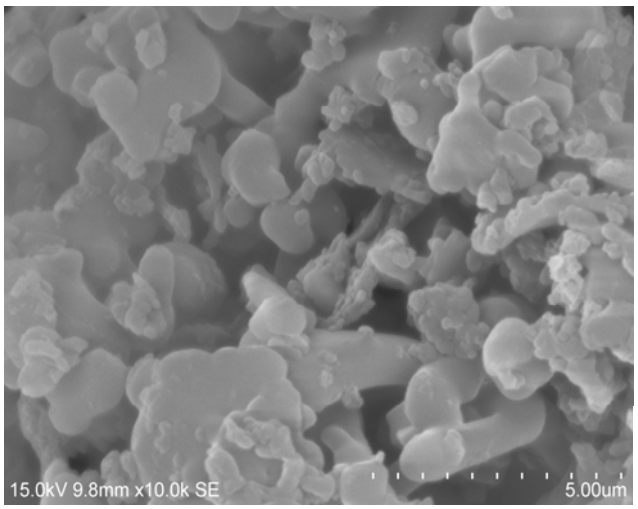

Figure 5: SEM Micrograph of PMAP

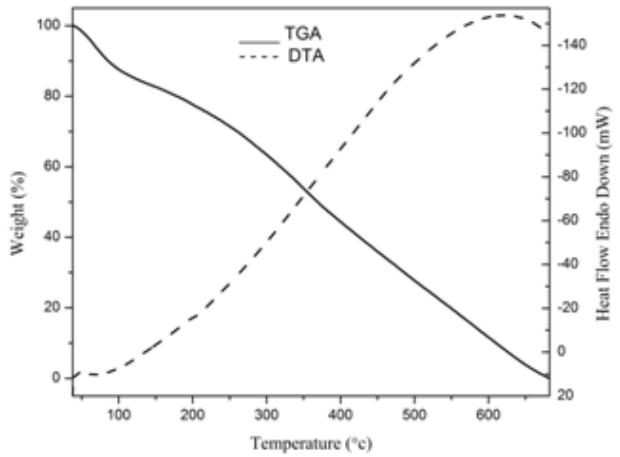

Figure 6: Thermo gravimetric patterns TGA and DTA of PMAP as a function of temperature

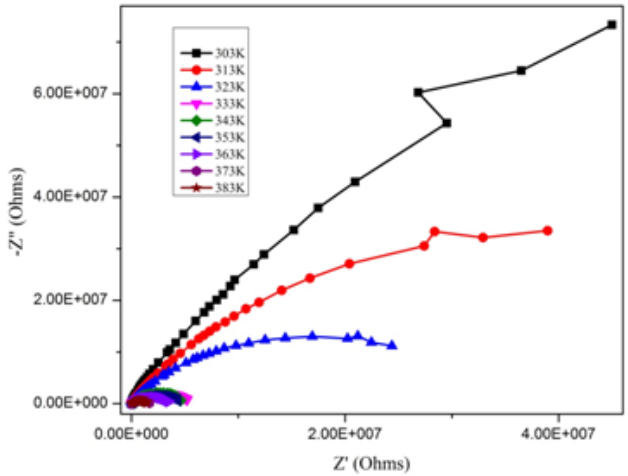

Figure 7: Complex Impedance plots of PMAP over the temperature range 303-383K

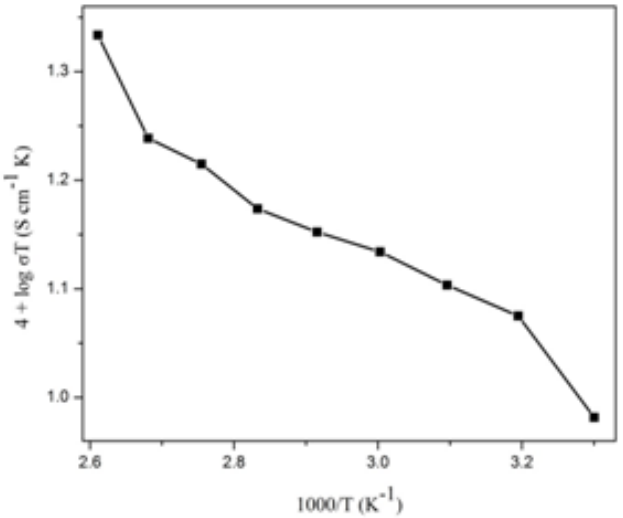

Figure 8: Temperature-dependent AC conductivity data of PMAP over the temperature range 303-383K

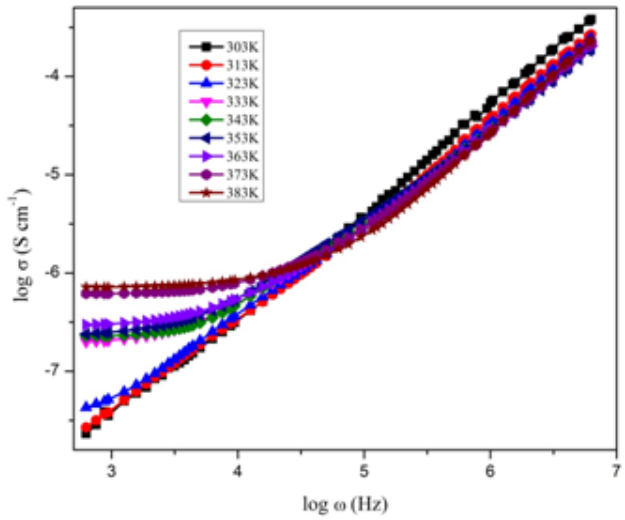

Figure 9: Frequency dependent AC conductivity (log σ vs log ω) plots of PMAP over the temperature range 303-383K

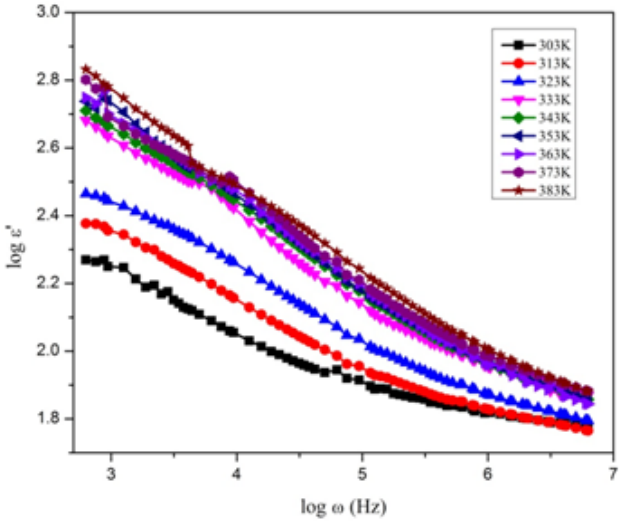

Figure 10a: Logarithmic plots of dielectric constant as a function of frequency for PMAP

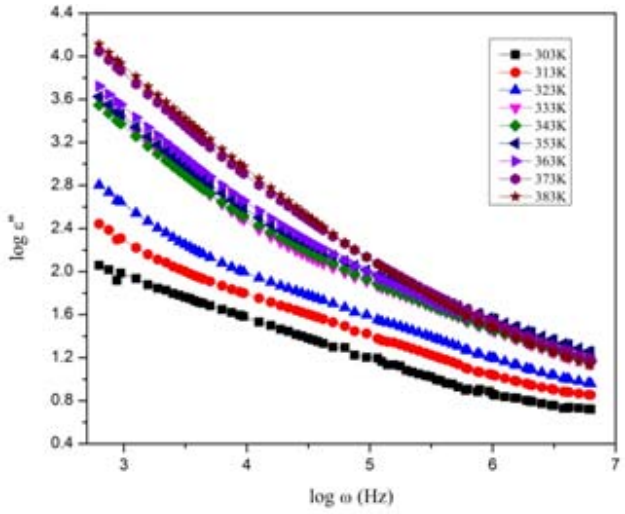

Figure 10b: Logarithmic plots of dielectric loss as a function of frequency for PMAP

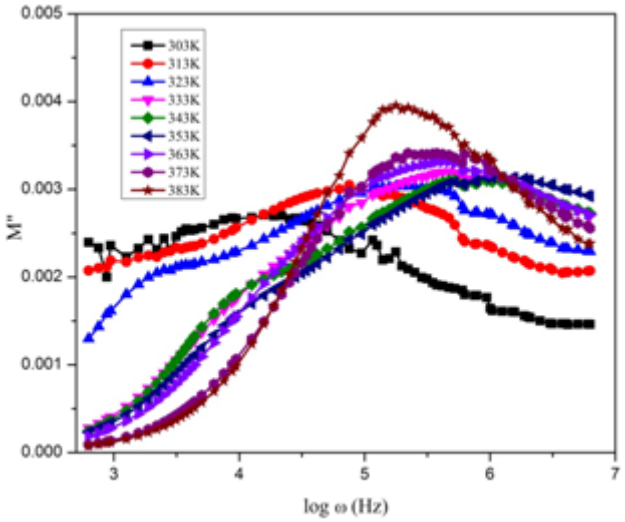

Figure 11a: Isothermal graphs of imaginary part of electric modulus for PMAP

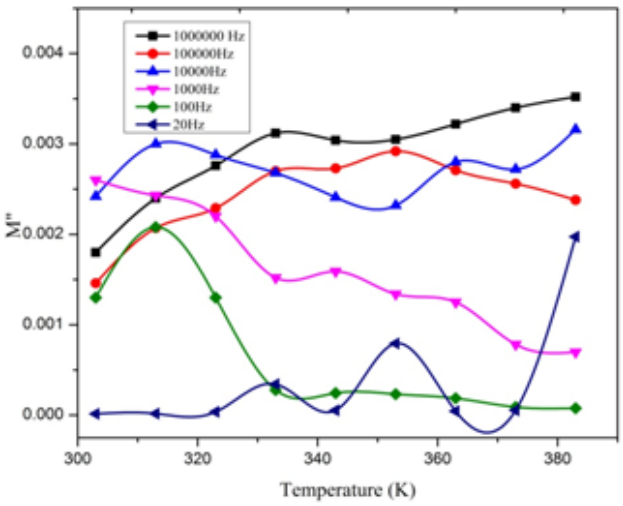

Figure 11b: Isochrones graphs of imaginary part of electric modulus for PMAP

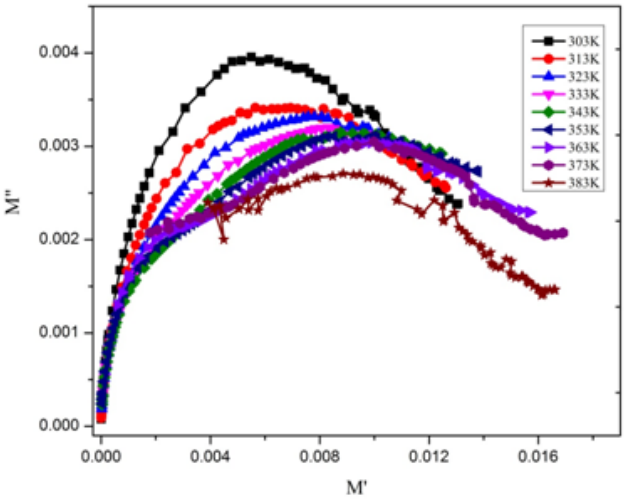

Figure 12: Complex planes for the electric modulus of PMAP at different temperatures

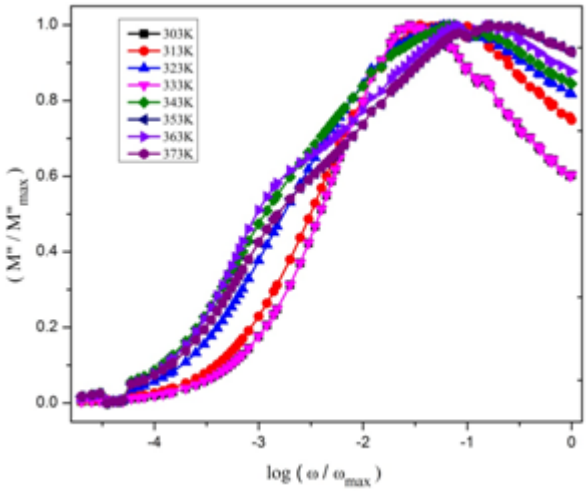

Figure 13: Normalized plots of M" / M"$_{max}$ Vs log (ω / ω_{max}) at different temperatures of PMAP

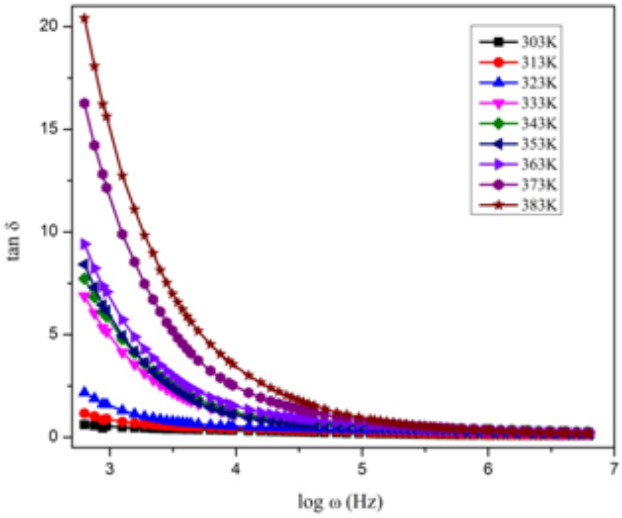

Figure 14: Frequency dependence of dissipation factor of PMAP